Trichostatin A

Subjects: Plant Sciences
Contributor: Suk Weon Kim

Trichostatin A (TSA) is a representative histone deacetylase (HDAC) inhibitor that modulates epigenetic gene expression by regulation of chromatin remodeling in cells.

Keywords: trichostatin A ; genome editing efficiency ; histone acetylation ; chromatin de-condensation ; plant protoplasts

1. Introduction

The CRISPR/Cas system is an efficient genome editing technology following meganucleases, zinc-finger nucleases (ZFNs), and transcription activator-like effector nucleases (TALENs) [1][2][3]. The CRISPR/Cas9 system, consisting of the Cas9 protein derived from *Streptococcus pyogenes* and gRNA, is the most widely used system based on RNA-guided interference with DNA [4]. The gRNA is a small RNA that contains 20 nucleotides complementary to target sequences and an artificial fusion of a crRNA and a fixed transactivating crRNA for recruiting the Cas9 protein to direct the cleavage of DNA sequences adjacent to 5′-NGG-3′ protospacer-adjacent motifs (PAMs) [5]. As a result, the Cas9 protein cleaves the target region in a sequence-dependent manner, and a double-strand break (DSB) is generated and repaired in that region, resulting in genome modification.

The CRISPR/Cas system is actively used for genome editing in a variety of species, including plants [6][7][8]. In particular, the Cas9 protein-gRNA ribonucleoproteins (RNPs) system has received attention for its ability to reduce the possibility of the insertion of recombinant DNA into the host genome [9]. Advances in CRISPR/Cas genome editing have accelerated the improvement of crop traits and have produced transgene-free genome-edited plants in a short time [7]. The application of this system has been reported in various plants such as Arabidopsis, tobacco, rice, and wheat [1][2][10]. Traits mainly related to productivity, biological and abiotic stress resistance, and nutritional quality improvement are being manipulated by genome editing. Therefore, the technology for developing genome editing crops using CRISPR/Cas will help to develop active alternatives in the fields of plant-related global issues, such as strengthening the global food supply, responding to global warming, and sustainable agriculture.

To promote the efficiency of genome-edited plant development, there are three major ways to increase the efficiency of genome editing: efficient gRNA design, effective delivery systems, and increased gRNA accessibility to the target region through chromatin structural modification. In recent years, active research has been conducted on guidelines and software tools for effective CRISPR gRNA design [11][12][13]. The computational approaches have been developed for scoring guide RNAs to escape low cleavage efficiency and off-target effects [10]. Furthermore, the delivery of editing reagents to plant cells is a very critical step for the generation of genome-edited plants. Protoplast transfection, *Agrobacterium*-mediated transfer DNA (T-DNA) transformation, or particle bombardment are methods by which CRISPR-mediated editing reagents, including DNA, RNA, and RNPs can be delivered to plant cells. Direct transfection into the protoplast is used for the regeneration of transgene-free genome-edited plants, whereas *Agrobacterium*-mediated transformation and particle bombardment are normally used for the two major vector delivery methods for the production of edited plants [14]. Advances in efficient delivery systems will accelerate plant genome editing in the future. Lastly, increasing the efficiency of genome editing can be achieved by increased gRNA accessibility to the target region through chromatin structure. It was reported that the treatments of chromatin-modulating compounds induce histone hyperacetylation at the target sites, resulting in a significant increase in the efficiency of indel formation in a dose-response manner in mammalian cells [15]. In particular, it is known that TSA is effective in animal cells, but its effect has not been proven in plant cells.

Trichostatin A (TSA) is a representative histone deacetylase (HDAC) inhibitor that can bind to HDAC by inserting its long aliphatic chain into the catalytic active pocket, resulting in inhibition of the enzymatic activity of HDAC [16]. It was reported that TSA facilitates totipotency in the male gametophyte in *Brassica napus* [17], and HDAC inhibitors TSA and suberoylanilide hydroxamic acid (SAHA) improved the rate of microspore embryogenesis and the frequency of direct plant regeneration in pakchoi (*Brassica rapa* ssp. *chinensis* L.) [18]. Wheat microspore-derived embryogenesis and green plant

regeneration were similarly activated by TSA treatment, suggesting that TSA leads to an increase in histone acetylation and global alteration of gene expression [19]. However, TSA's effects on the genome editing efficiency of CRISPR/Cas9 have been not examined in plant protoplasts.

2. Effects of TSA on Genome Editing Efficiency Using Cas9 Transfection from Protoplasts

We tested whether a compound for epigenetic regulation, TSA, plays a stimulatory role in CRISPR/Cas9 genome editing during PEG transfection, especially by leading to chromatin structural modification. To prove this hypothesis, first of all, we selected the lettuce *SOC1* gene and tobacco *PDS* gene as targets for genome editing from protoplasts. We designed the gRNA of the lettuce *SOC1* gene using CRISPR RGEN Tools (http://www.rgenome.net/cas-designer/) (**Figure 1**A) and the gRNA of the tobacco *PDS* gene by referring to the previous study for gRNA design. To investigate whether gRNA works properly, we examined whether it was cleaved under in vitro conditions. It was confirmed that Cas9–RNP complexes from lettuce were cleaved well at their target sites in the in vitro cleavage assay (**Figure 1**B).

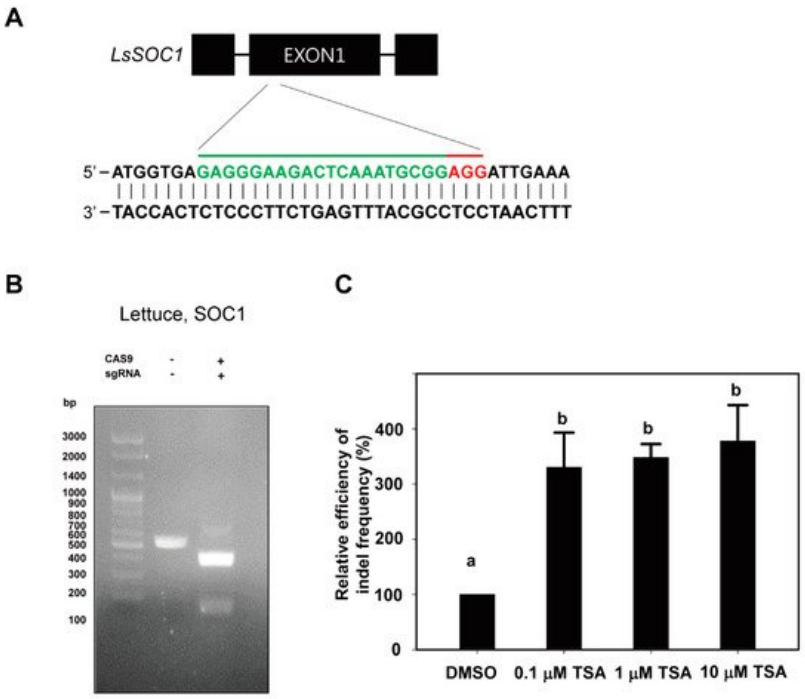

Figure 1. Changes in indel frequency according to TSA treatment in lettuce protoplasts. (**A**) Schematic illustration of the *LsSOC1* CRISPR/Cas9 target site. The target region is shown in green letters followed by PAM (NGG; red). (**B**) In vitro DNA cleavage assay using *LsSOC1* gRNA and Cas9 protein. The gRNA-mediated cleavage of target DNA in vitro is shown in agarose gel. The 546bp PCR fragment of the *LsSOC1* gene is used as a substrate for gRNA-Cas9 digestion. *LsSOC1* gRNA leads to a specific digestion of the target DNA, producing DNA fragments of 386 bp and 160 bp. (**C**) Relative efficiency of indel frequency (%) of at target site in protoplasts examined at 48 h after transfection of Cas9 and gRNAs as RNP complexes with DMSO or TSA treatment. The indel frequency of the DMSO treatment group was set to 100%, and those of the TSA treatment groups are shown relatively. Bars represent means ± SE (n = 3) of independent experiments. Different letters on the bars indicate significant differences between each treatment (ANOVA with the Duncan's test, $p < 0.05$).

To examine the effects of TSA, an inhibitor of HDACs, on genome editing efficiency of plant protoplasts with the Cas9 protein-gRNA RNP system, TSA was treated with different concentrations (0, 0.1, 1 and 10 μM) of freshly isolated protoplasts of lettuce immediately after PEG transfection. In the case of tobacco protoplasts, TSA was treated in the same manner as lettuce without 10 μM TSA treatment. TSA treatment significantly enhanced the indel frequency from lettuce protoplasts compared to DMSO treatment (**Figure 1**C and **Table 1**). In comparison with DMSO, TSA increased the indel frequency by 330%, 348% and 378% at concentrations of 0.1, 1 and 10 μM, respectively (**Figure 1**C). The indel frequency showed more than a three-times increase in all TSA treatments regardless of concentrations. The indel frequencies at the target site of *LsSOC1* gRNA for DMSO, 0.1, 1 and 10 μM TSA treatment were in the range of 0.9–2.7%, 4.0–8.6%, 3.4–9.9% and 4.5–9.6%, respectively. Although the indel frequencies differed in each experiment, the relative efficiencies of indel frequency showed a similar pattern in all three repeated experiments (**Table 1**). These results clearly represented that TSA has a stimulatory role in CRISPR/Cas9 editing. However, this was observed at a very low indel frequency in the only Cas9 protein without *LsSOC1* gRNA treatment.

Table 1. Summary of the indel frequencies based on deep sequencing analysis of *LsSOC1* target region from lettuce protoplasts. Each treatment consisted of three repeats, and average and standard deviation are represented. The superscripts in indel frequency indicate significant differences between each treatment (ANOVA with the Duncan's test, $p < 0.05$).

Plant Species	Concentration of TSA (μM)	Total Reads	WT	Insertions	Deletions	Indel Frequency (%)
L. sativa	0 (DMSO)	54,379 ± 3823	53,427 ± 4239	788 ± 283	165 ± 128	1.8 ± 0.9 [a]
	0.1	50,396 ± 1629	47,864 ± 16,395	2179 ± 93	353 ± 126	5.6 ± 2.6 [b]
	1	55,397 ± 20,223	52,292 ± 16,785	2677 ± 571	428 ± 176	6.2 ± 3.2 [b]
	10	53,667 ± 3833	50,610 ± 20,077	2639 ± 322	419 ± 101	6.4 ± 2.8 [b]

Similar to lettuce protoplasts, the stimulatory effect of TSA on the increase in the indel frequency also showed a similar pattern to that of tobacco protoplasts. Treatment with 0.1 μM TSA and 1uM TSA increased the indel frequency by 149% and 184%, respectively, compared to DMSO control treatment. Although the increase in indel frequency was lower than that of lettuce, it was found that the indel frequency increased with 1 μM TSA treatment with statistical significance. A full list of the detected mutations is provided in the Supplementary excel data. After combining the results from the lettuce and tobacco protoplasts, we suggest that TSA treatment increases genome editing efficiency using plant protoplasts with the Cas9-RNP system.

3. Effects of TSA on the Mutation Patterns in Protoplast Cultures

Next, we analyzed the indel patterns induced by Cas9–RNP complexes with TSA treatment. Interestingly, TSA has not only increased the indel frequency but also induced more various indel mutation patterns from lettuce protoplasts (**Figure 2**). In the case of DMSO treatment, the indel mutation patterns at the target site of the *LsSOC1* gRNA were 41, but those of 0.1, 1 and 1 μM TSA were 105, 138 and 121, respectively (**Figure 2**). These results clearly show that TSA has a stimulatory role in the increase in indel mutation patterns from lettuce protoplasts using *LsSOC1* gRNA. The results suggest that TSA treatment induces more cleavage of the target by the Cas9 protein-gRNA RNPs, resulting in more mutations. An insertion of one base pair was the most common editing pattern among mutation patterns at the *LsSOC1* target loci in protoplasts treated with DMSO or TSA but showing a difference in mutation number (**Figure 3**). For example, in the case of 1 bp insertion, T insertion of target site, 0.1 μM, 1 μM and 10 μM TSA treatment yielded 1346, 1776 and 1770 reads, respectively, while DMSO treatment yielded 556 reads. Furthermore, different types of 1 bp insertions, A and G insertion, and short deletion are mainly found at the *LsSOC1* target loci in protoplasts treated with DMSO or TSA. The results are consistent with a previous study in which mutations caused by Cas9 during DSB repair were predominantly short deletions and 1 bp insertions [10][20]. The data suggest that although TSA treatment can lead to a variety of patterns, the main patterns are similar and lead to differences in the indel frequency.

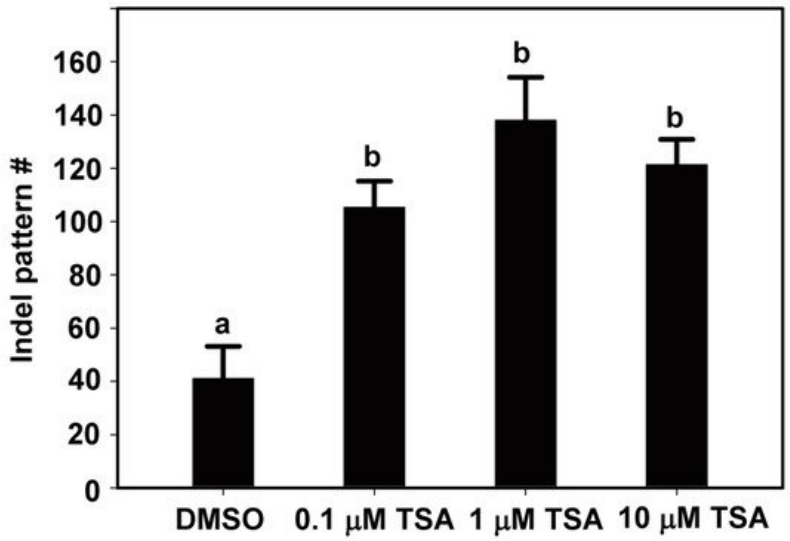

Figure 2. The number of indel patterns at the *LsSOC1* target loci in protoplasts examined at 48 h after transfection of Cas9 protein and gRNAs as RNP complexes with DMSO or TSA treatment. The total number of various indel patterns according to TSA treatment was analyzed by targeted deep sequencing.

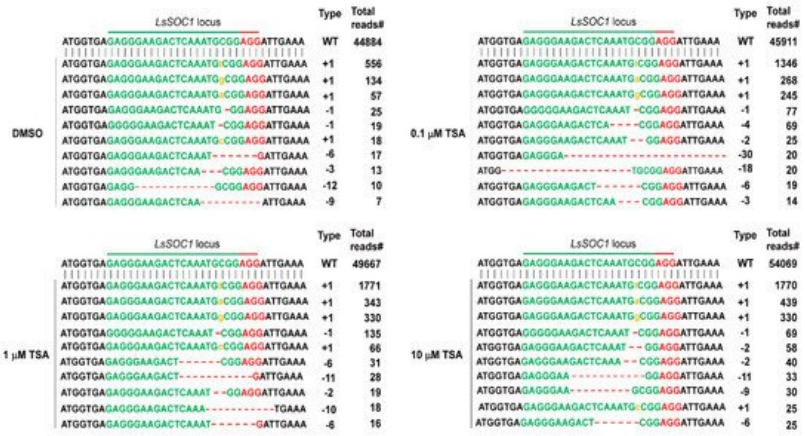

Figure 3. The representative indel types at *LsSOC1* target loci generated by delivery of Cas9 and gRNAs with DMSO or various concentrations of TSA treatment. An insertion of one base pair was the most common mutation pattern among the indel patterns induced by DMSO or various concentrations of TSA treatment at the *LsSOC1* loci. The target region is shown in green letters followed by PAM (NGG; red). Yellow lower-case letters mean inserted base, and red dash means nucleotide deletion.

4. Effects of TSA on the Structural Changes of Chromatin in Protoplast Cultures

Since the packaging of eukaryotic DNA into chromatin restricts the ability of the Cas9 protein and gRNA to access their target and the recruitment of DNA damage repair machinery to DNA DSB sites cleaved by Cas9, the potential relationships between chromatin remodeling and genome editing have been explored in many organisms, from yeast to humans [21][22][23][24]. Accordingly, we investigated the effects of TSA on chromatin structure by a chromatin accessibility test using micrococcal nuclease (MNase) that cuts internucleosomal DNA. The ratios of intact genomic band intensities treated with different concentrations of MNase (g_c) to the non-treated control (g_0) represent the degree of chromatin relaxation. It can be seen that the higher the concentration of MNase in the DMSO-treated group, the lower the ratio of g_c/g_0 (**Figure 4**). Chromatin accessibility of TSA treatment groups was higher than that of DMSO treatment group, as revealed by the lower g_0/g_c ratio. When treated with 1 units/mL MNase, the ratio decreased significantly according to the TSA concentration, which means that chromatin accessibility was higher. Although the difference between the TSA and DMSO treatment groups was small when 5 and 10 Units/mL MNase were treated, the ratio of g_c/g_0 of the TSA-treated group was lower than that of the DMSO-treated group, which means that chromatin accessibility was higher. These results indicate that TSA has a positive effect on the chromatin structural modification in protoplasts and may influence the ability of gRNA to access the target or the recruitment of DNA damage repair machinery to DNA DSB cleaved by Cas9 after PEG transfection.

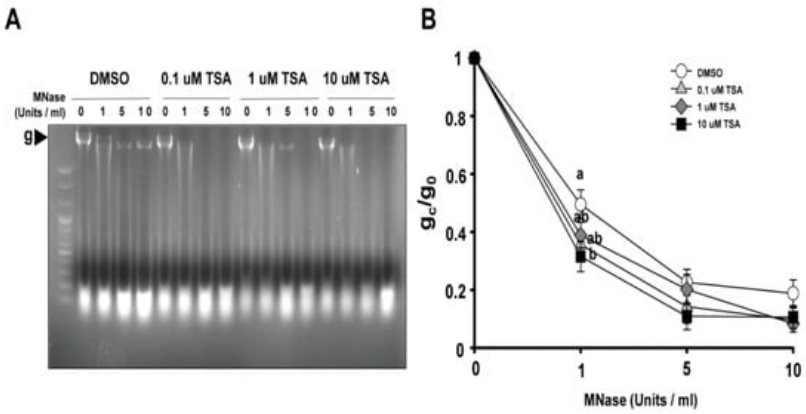

Figure 4. The effect of TSA on chromatin structures in lettuce protoplasts. (**A**) Representative image of chromatin digestion with micrococcal nuclease (MNase). The genomic band intensities with different concentrations of TSA were examined. The arrow means the genomic band without and with treatment with different concentrations of MNase. (**B**) Proportion of MNase-digested chromatin DNA resolved on agarose gels. The genomic band intensities without (g_0) and

with (g_c) treatment with different concentrations of MNase were quantified, and the ratio of g_c/g_0 was used to represent the degree of chromatin relaxation. Bars represent means ± SE (n = 5) of independent experiments. Different letters on the bars indicate significant differences between each treatment (ANOVA with Duncan's test, $p < 0.05$).

5. Effects of TSA on Histone Acetylation in Protoplast Cultures

It was reported that TSA causes an increase in global histone H3 and H4 acetylation in plants [14][17][25][26]. To investigate the effect of TSA on histone acetylation in protoplast conditions, Western blot analysis with H3 and H4 acetylation antibodies and H3 and H4 antibodies was carried out in lettuce protoplasts after TSA treatments (**Figure 5**). After 6 and 12 h of TSA treatments, histone H3 and H4 acetylation in lettuce protoplasts was significantly increased compared to that in the control, and this increase was concentration-dependent. These results indicate that the level of histone H3 and H4 acetylation was increased by TSA from lettuce protoplasts.

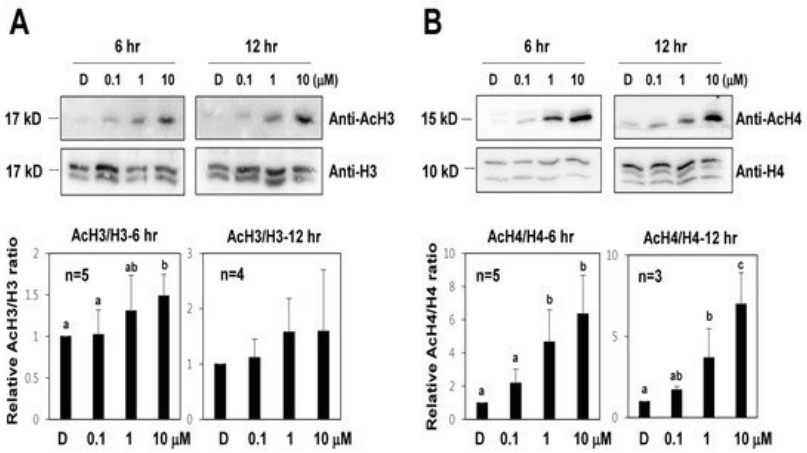

Figure 5. The effect of TSA on histone H3 and H4 acetylation level in lettuce protoplasts. Total protein extracts were obtained from lettuce protoplasts after 6 or 12 h after TSA treatments. Error bars represent SD (n = 3 or more). (**A**) H3 Histone acetylation levels were determined with a Western blot using an anti-H3 and anti-AcH3 antibody. (**B**) H4 histone acetylation levels were determined with a Western blot using an anti-H4 and anti-AcH4 antibody. Different letters on the bars indicate significant differences between each treatment. H3 = histone H3 antibody; AcH3 = acetylated histone H3 antibody; H4 = histone H4 antibody; AcH4 = acetylated histone H4 antibody.

6. Effects of TSA on Expression of Cell Division Regulatory Genes and Formation of Callus

We have already demonstrated that TSA has a stimulatory role in increasing the efficiency of genome editing from protoplasts. Initial cell division and callus formation from protoplast are essential steps for the development of genome-edited plants using the CRISPR/Cas9 RNP system. In order for TSA to be used as a positive stimulator for the development of genome-edited plants, its effect on subsequent cell division and callus formation from protoplasts must be investigated. If TSA prevents subsequent cell division and callus formation from protoplasts, it cannot be used as a positive stimulator for the development of genome-edited plants. Thus, we first checked how TSA treatment affects cell division-related gene expression from lettuce protoplasts. The quantitative reverse transcription PCR (qRT-PCR) analysis showed that the transcripts levels of *LsCYCD1-1*, *LsCYCD3-2*, *LsCYCD6-1*, and *LsCYCU4-1* were increased by TSA treatment, except for *LsKRP3* (**Figure 6**). Overall, when a high concentration of TSA (10 μM) was treated, cell division-related gene expression was also significantly increased. Compared to the high-concentration TSA treatment, the gene expression was decreased in the low-concentration (0.1 μM) TSA treatment. These results show that the TSA-induced increase in gene expression occurs in a concentration-dependent manner. On the other hand, there was no statistically significant difference in the expression of the cell division inhibitor *KRP3* gene by TSA treatment. Considering these results, we suggest that TSA treatment has a positive effect on the expression of cell division-related genes as well as genome editing efficiency from lettuce protoplasts.

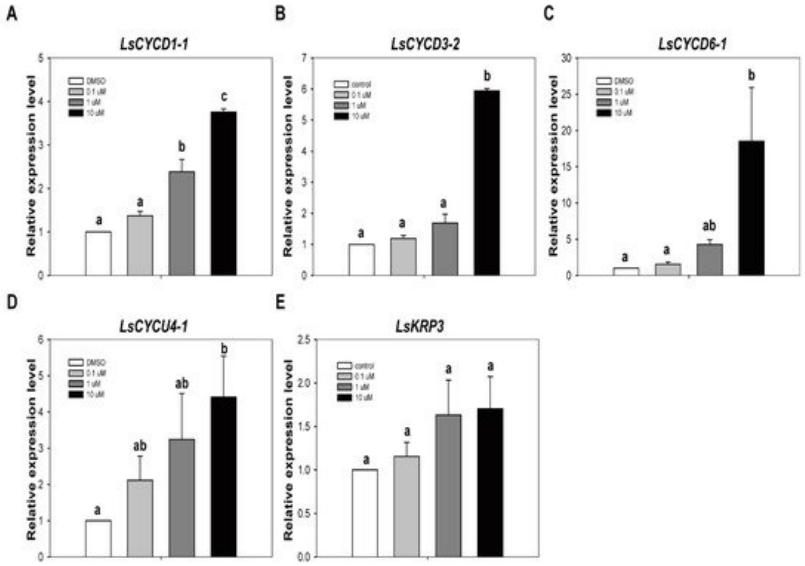

Figure 6. The effect of TSA on expression of cell division regulatory genes. The relative gene expression level of *LsCYCD1-1* (**A**), *LsCYCD3-2* (**B**), *LsCYCD6-1* (**C**), *LsCYCU4-1* (**D**) and *LsKRP3* (**E**) in lettuce protoplasts. qRT-PCR was performed with total RNA extracted from lettuce protoplasts after treatment with DMSO or TSA for 12 hr. Bars represent means ± SE (n = 3) of independent experiments. Different letters on the bars indicate significant differences between each treatment (ANOVA with Duncan's test, $p < 0.05$).

Next, we observed the effects of TSA on callus proliferation from Cas9-transfected tobacco protoplasts. Tobacco protoplasts are actively divided and easily form calluses, making them suitable for checking the effects of TSA treatment during plant regeneration. The green calluses were derived from tobacco protoplasts grown for approximately 5 weeks in a callus induction medium. Callus proliferation from non-transfected tobacco protoplasts was significantly enhanced upon TSA treatment; the size of callus clumps was increased strikingly by treatment with 1 µM TSA. Interestingly, treatment with TSA at 1 µM concentrations also promoted callus proliferation from transfected tobacco protoplasts compared to the control, although not as much as in the case of untreated protoplasts. In addition, *PDS* gene-edited tobacco plants with an albino phenotype were obtained from the green callus. The result suggests that TSA treatment promotes callus proliferation from the transfected or non-transfected tobacco protoplasts as well as genome editing efficiency.

References

1. Shan, Q.; Wang, Y.; Li, J.; Zhang, Y.; Chen, K.; Liang, Z.; Zhang, K.; Liu, J.; Xi, J.J.; Qiu, J.L.; et al. Targeted genome modification of crop plants using a CRISPR-Cas system. Nat. Biotechnol. 2013, 31, 686–688.
2. Nekrasov, V.; Staskawicz, B.; Weigel, D.; Jones, J.D.; Kamoun, S. Targeted mutagenesis in the model plant Nicotiana benthamiana using Cas9 RNA-guided endonuclease. Nat. Biotechnol. 2013, 31, 691–693.
3. Li, J.F.; Norville, J.E.; Aach, J.; McCormack, M.; Zhang, D.; Bush, J.; Church, G.M.; Sheen, J. Multiplex and homologous recombination-mediated genome editing in Arabidopsis and Nicotiana benthamiana using guide RNA and Cas9. Nat. Biotechnol. 2013, 31, 688–691.
4. Koonin, E.V.; Makarova, K.S.; Zhang, F. Diversity, classification and evolution of CRISPR-Cas systems. Curr. Opin. Microbiol. 2017, 37, 67–78.
5. Jiang, F.; Doudna, J.A. CRISPR–Cas9 Structures and Mechanisms. Annu. Rev. Biophys. 2017, 46, 505–529.
6. Li, H.; Yang, Y.; Hong, W.; Huang, M.; Wu, M.; Zhao, X. Applications of genome editing technology in the targeted therapy of human diseases: Mechanisms, advances and prospects. Signal Transduct. Target. Ther. 2020, 5, 1.
7. Manghwar, H.; Lindsey, K.; Zhang, X.; Jin, S. CRISPR/Cas System: Recent Advances and Future Prospects for Genome Editing. Trends Plant Sci. 2019, 24, 1102–1125.
8. Lino, C.A.; Harper, J.C.; Carney, J.P.; Timlin, J.A. Delivering CRISPR: A review of the challenges and approaches. Drug Deliv. 2018, 25, 1234–1257.
9. Woo, J.W.; Kim, J.; Kwon, S.I.; Corvalan, C.; Cho, S.W.; Kim, H.; Kim, S.G.; Kim, S.T.; Choe, S.; Kim, J.S. DNA-free genome editing in plants with preassembled CRISPR-Cas9 ribonucleoproteins. Nat. Biotechnol. 2015, 33, 1162–1164.
10. Wada, N.; Ueta, R.; Osakabe, Y.; Osakabe, K. Precision genome editing in plants: State-of-the-art in CRISPR/Cas9-based genome engineering. BMC Plant Biol. 2020, 20, 234.

11. Sledzinski, P.; Nowaczyk, M.; Olejniczak, M. Computational Tools and Resources Supporting CRISPR-Cas Experiments. Cells 2020, 9, 1288.
12. Wang, D.; Zhang, C.; Wang, B.; Li, B.; Wang, Q.; Liu, D.; Wang, H.; Zhou, Y.; Shi, L.; Lan, F.; et al. Optimized CRISPR guide RNA design for two high-fidelity Cas9 variants by deep learning. Nat. Commun. 2019, 10, 4284.
13. Bradford, J.; Perrin, D. A benchmark of computational CRISPR-Cas9 guide design methods. PLoS Comput. Biol. 2019, 15, e1007274.
14. Chen, K.; Wang, Y.; Zhang, R.; Zhang, H.; Gao, C. CRISPR/Cas Genome Editing and Precision Plant Breeding in Agriculture. Annu. Rev. Plant Biol. 2019, 70, 667–697.
15. Chakrabarti, A.M.; Henser-Brownhill, T.; Monserrat, J.; Poetsch, A.R.; Luscombe, N.M.; Scaffidi, P. Target-Specific Precision of CRISPR-Mediated Genome Editing. Mol. Cell 2019, 73, 699–713 e6.
16. Zhang, H.; Wang, B.; Duan, C.G.; Zhu, J.K. Chemical probes in plant epigenetics studies. Plant Signal. Behav. 2013, 8, e25364.
17. Li, H.; Soriano, M.; Cordewener, J.; Muino, J.M.; Riksen, T.; Fukuoka, H.; Angenent, G.C.; Boutilier, K. The histone deacetylase inhibitor trichostatin a promotes totipotency in the male gametophyte. Plant Cell 2014, 26, 195–209.
18. Zhang, L.; Zhang, Y.; Gao, Y.; Jiang, X.; Zhang, M.; Wu, H.; Liu, Z.; Feng, H. Effects of histone deacetylase inhibitors on microspore embryogenesis and plant regeneration in Pakchoi (Brassica rapa ssp. chinensis L.). Sci. Hortic. 2016, 209, 61–66.
19. Jiang, F.; Ryabova, D.; Diedhiou, J.; Hucl, P.; Randhawa, H.; Marillia, E.F.; Foroud, N.A.; Eudes, F.; Kathiria, P. Trichostatin A increases embryo and green plant regeneration in wheat. Plant Cell Rep. 2017, 36, 1701–1706.
20. Pathak, B.; Zhao, S.; Manoharan, M.; Srivastava, V. Dual-targeting by CRISPR/Cas9 leads to efficient point mutagenesis but only rare targeted deletions in the rice genome. 3 Biotech. 2019, 9, 158.
21. Yarrington, R.M.; Verma, S.; Schwartz, S.; Trautman, J.K.; Carroll, D. Nucleosomes inhibit target cleavage by CRISPR-Cas9 in vivo. Proc. Natl. Acad. Sci. USA 2018, 115, 9351–9358.
22. Savell, K.E.; Day, J.J. Applications of CRISPR/Cas9 in the Mammalian Central Nervous System. Yale J. Biol. Med. 2017, 90, 567–581.
23. Pulecio, J.; Verma, N.; Mejia-Ramirez, E.; Huangfu, D.; Raya, A. CRISPR/Cas9-Based Engineering of the Epigenome. Cell Stem Cell 2017, 21, 431–447.
24. Isaac, R.S.; Jiang, F.; Doudna, J.A.; Lim, W.A.; Narlikar, G.J.; Almeida, R. Nucleosome breathing and remodeling constrain CRISPR-Cas9 function. eLife 2016, 5, e13450.
25. Wang, J.; Tian, C.; Zhang, C.; Shi, B.; Cao, X.; Zhang, T.Q.; Zhao, Z.; Wang, J.W.; Jiao, Y. Cytokinin Signaling Activates WUSCHEL Expression during Axillary Meristem Initiation. Plant Cell 2017, 29, 1373–1387.
26. Mengel, A.; Ageeva, A.; Georgii, E.; Bernhardt, J.; Wu, K.; Durner, J.; Lindermayr, C. Nitric Oxide Modulates Histone Acetylation at Stress Genes by Inhibition of Histone Deacetylases. Plant Physiol. 2017, 173, 1434–1452.